Hindawi Publishing Corporation
EURASIP Journal on Advances in Signal Processing
Volume 2007, Article ID 75621, 12 pages
doi:10.1155/2007/75621

Research Article

Subband Affine Projection Algorithm for Acoustic Echo Cancellation System

Hun Choi and Hyeon-Deok Bae

Department of Electronic Engineering, Chungbuk National University, 12 Gaeshin-Dong, Heungduk-Gu, Cheongju 361-763, South Korea

Received 30 December 2005; Revised 14 April 2006; Accepted 18 May 2006

Recommended by Yuan-Pei Lin

We present a new subband affine projection (SAP) algorithm for the adaptive acoustic echo cancellation with long echo path delay. Generally, the acoustic echo canceller suffers from the long echo path and large computational complexity. To solve this problem, the proposed algorithm combines merits of the affine projection (AP) algorithm and the subband filtering. Convergence speed of the proposed algorithm is improved by the signal-decorrelating property of the orthogonal subband filtering and the weight updating with the prewhitened input signal of the AP algorithm. Moreover, in the proposed algorithms, as applying the polyphase decomposition, the noble identity, and the critical decimation to subband the adaptive filter, the sufficiently decomposed SAP updates the weights of adaptive subfilters without a matrix inversion. Therefore, computational complexity of the proposed method is considerably reduced. In the SAP, the derived weight updating formula for the subband adaptive filter has a simple form as ever compared with the normalized least-mean-square (NLMS) algorithm. The efficiency of the proposed algorithm for the colored signal and speech signal was evaluated experimentally.

1. INTRODUCTION

Adaptive filtering is essential for acoustic echo cancellation. Among the adaptive algorithms, least-mean-square (LMS) is the most popular algorithm for its simplicity and stability. However, when the input signal is highly correlated and the long-length adaptive filter is needed, the convergence speed of the LMS adaptive filter can be deteriorated seriously [1, 2]. To overcome this problem, the affine projection (AP) algorithm was proposed [3–11]. The improved performance of the AP algorithm is characterized by an updating-projection scheme of an adaptive filter on a P-dimensional data-related subspace. Since the input signal is prewhitened by this projection on an affine subspace, the convergence rate of the AP adaptive filter is improved. However, a large computational complexity is a major drawback for its implementation, because P-ordered AP adaptive filter is based on the data matrix that consists of the last $P+1$ input vectors and it requires matrix inversion in weight updating.

The orthogonal subband filtering (OSF) is an alternative method that can whiten the input signal [12–15]. The OSF can be considered a kind of projection operation. It is similar in the view of decorrelating property to the affine projection scheme. Therefore, in subband structure with orthogonal analysis filter banks, the convergence speed of the subband adaptive filter (SAF) is improved by the weight updating with prewhitened inputs that result from the OSF. Recently, for fast convergence and efficient implementation, there has been increasing interest in the combining advantages of the AP and the SAF [16–21]. These algorithms, for reducing computational complexity, are based on the fast variant of AP (FAP) instead of the conventional AP. The FAP-based algorithms use various iterative methods to avoid the matrix inversion in weight updating. However, in the FAP-based algorithms, the performances are deteriorated by the approximated errors of the iterative method and the computational complexity is still complex for the implementation.

In this paper, we present a new subband affine projection (SAP) algorithm to improve convergence speed and reduce computational complexity of the AP algorithm. The SAP is based on the subband structure [13] that uses critically decimated adaptive filters with the polyphase decomposition and the noble identity. A new criterion is also presented for applying AP algorithm to polyphase decomposed adaptive filter

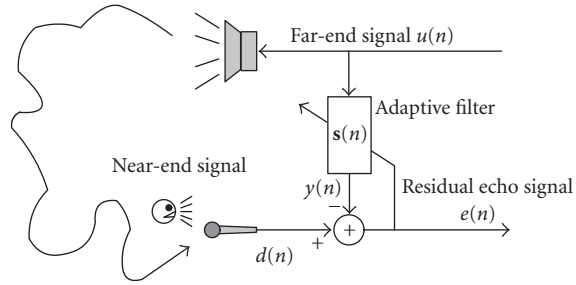

(a) Fullband adaptive acoustic echo canceller

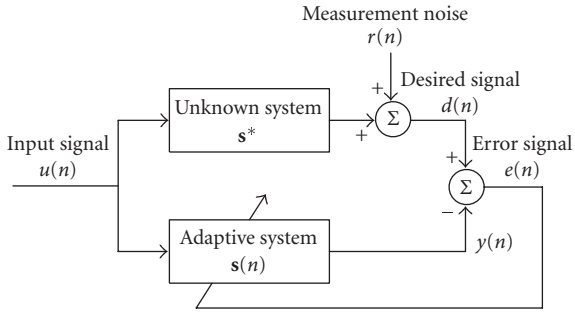

(b) Fullband adaptive system identification

Figure 1: Fullband system identification for adaptive acoustic echo canceller.

(adaptive subfilter) in each subband. In this algorithm, the derived weight updating formula for the subband adaptive filter has a simple form as compared with the normalized least-mean-square (NLMS) algorithm, and the weights of the adaptive subfilter are updated with the input prewhitened by the OSF in each subband. To evaluate the performance of the proposed SAP, computer simulations are performed for system identification model of echo cancellation problem.

The outline of this paper is as follows. In Section 2, the conventional AP algorithm is reviewed. In Section 3, we derive the new subband affine projection algorithm and describe the convergence analysis and computational complexity of the proposed algorithm. Section 4 describes simulation results, and Section 5 contains the conclusions.

2. AFFINE PROJECTION ALGORITHM

Consider the adaptive acoustic echo cancellation (AEC) system and the block diagrams of system identification for the AEC in fullband structure as shown in Figure 1. In Figure 1(b), the adaptive filter attempts to estimate a desired signal $d(k)$ which is linearly related to the input signal $u(k)$ by model

$$d(k) = \mathbf{s}^{*T}\mathbf{u}(k) + r(k), \tag{1}$$

where $\mathbf{s}^*$ is the echo path that we wish to estimate and $r(k)$ is the measurement noise that is the independent identically distributed (i.i.d.) random signal with zero mean and variance σ_r^2. The input signal $u(k)$ is assumed to be a zero-mean wide-sense stationary (WSS) autoregressive (AR) process of order P, then the input signal $u(k)$ is described by

$$u(k) = \sum_{l=1}^{P} a_l u(k-l) + f(k), \tag{2}$$

where $f(k)$ is a WSS white process with variance σ_f^2. Let $\mathbf{u}(k)$ be a vector of N samples of AR process described in (3), we can rewrite the AR signal as

$$\mathbf{u}(k) = \sum_{l=1}^{P} a_l \mathbf{u}(k-l) + \mathbf{f}(k) = \mathbf{U}_a(k)\mathbf{a} + \mathbf{f}(k), \tag{3}$$

where the matrices $\mathbf{U}_a(k) = [\mathbf{u}(k-1)\ \ \mathbf{u}(k-2)\ \cdots\ \mathbf{u}(k-P)]$, $\mathbf{u}(k-l) = [u(k-l)\ \ u(k-l-1)\ \cdots\ u(k-l-N+1)]^T$ and, $\mathbf{f}(k) = [f(k)\ \ f(k-1)\ \cdots\ f(k-N+1)]^T$.

In the system identification for the fullband AEC as shown in Figure 1(b), $y(k)$ is the output signal of the adaptive filter at iteration k. The error signal is defined by $e(k) = d(k) - y(k)$. The P-order AP adaptive filter uses $(P+1)\times N$ data matrix and the optimization criterion for designing the adaptive filter is given by [2, 22],

$$\begin{aligned} &\text{minimize } \left|\left|\mathbf{s}(k+1) - \mathbf{s}(k)\right|\right|^2 \\ &\text{subject to } \mathbf{d}(k) = \mathbf{U}^T(k)\mathbf{s}(k+1), \end{aligned} \tag{4}$$

where

$$\begin{aligned} \mathbf{U}(k) &= \left[\mathbf{u}(k)\ \ \mathbf{u}(k-1)\mathbf{u}(k-2)\ \cdots\ \mathbf{u}(k-P)\right] \\ &= \left[\mathbf{u}(k)\ \ \mathbf{U}_a(k)\right]. \end{aligned} \tag{5}$$

It is well known that the AP algorithm is the undetermined optimization problem. Generally, Lagrangian theory is used for solving this optimization problem with equality constraints [2, 22, 23]. From (4), the weights of the adaptive filter are updated by the AP algorithm as in

$$\begin{aligned} \mathbf{s}(k+1) &= \mathbf{s}(k) + \mu\mathbf{U}(k)\left[\mathbf{U}(k)^T\mathbf{U}(k)\right]^{-1}\mathbf{e}(k), \\ \mathbf{e}(k) = \mathbf{d}(k) - \mathbf{y}(k) &= \left[e(k)\ \ e(k-1)\ \cdots\ e(k-P)\right]^T, \\ \mathbf{d}(k) = \mathbf{U}(k)^T\mathbf{s}^* &= \left[d(k)\ \ d(k-1)\ \cdots\ d(k-P)\right]^T, \\ \mathbf{y}(k) &= \mathbf{U}(k)^T\mathbf{s}(k). \end{aligned} \tag{6}$$

Parameters N and P are the length of the adaptive filter and the projection order, respectively. The step size μ is the relaxation factor. In P-order AP algorithm of (6), AR(P) input signal is decorrelated by the P times orthogonal projection operations with projection matrix as follows:

$$\mathbf{P}_{U_a}(k) = \mathbf{U}_a(k)\left[\mathbf{U}_a^T(k)\mathbf{U}_a(k)\right]^{-1}\mathbf{U}_a^T(k), \tag{7}$$

which achieves the projection operation onto the subspace spanned by the columns of $\mathbf{U}_a(k)$. Thus, the AP adaptive filter weights are updated by prewhitened input signals.

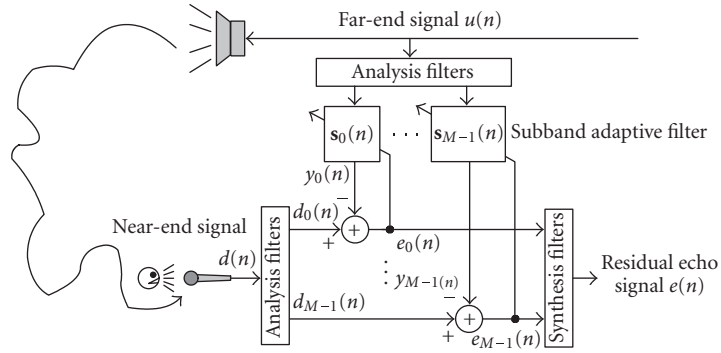

(a) Subband adaptive acoustic echo canceller

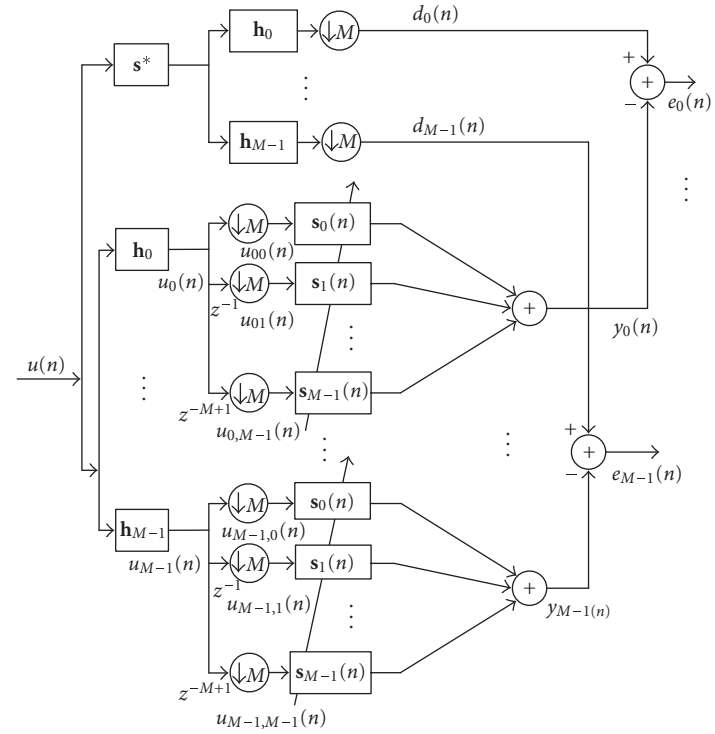

(b) Subband adaptive system identification

Figure 2: Subband system identification for adaptive acoustic echo canceller.

3. SUBBAND AFFINE PROJECTION ALGORITHM

Using polyphase decomposition and the noble identity [12], the fullband system of Figure 1 can be transformed into M-subband system [13]. Figure 2 shows the M-subband adaptive acoustic echo cancellation (SAEC) system and the block diagram of system identification for the SAEC. In [15], the excellency of this subband structure has been analyzed and is alias free, always stable, and reasonable for implementation. In Figure 2, using orthogonal analysis filters (OAFs) $\mathbf{h}_0 \ \cdots \ \mathbf{h}_{M-1}$, the input signal $u(k)$ and the desired signal $d(k)$ are partitioned into new signals denoted by $u_m(k)$ and $d_m(k)$, respectively. We can describe as

$$u_m(k) = \mathbf{h}_m^T\left[\mathbf{U}_{sa}(k)\mathbf{a} + \mathbf{f}_s(k)\right] = \mathbf{h}_m^T\mathbf{U}_{sa}(k)\mathbf{a} + f_m(k),$$
$$d_m(k) = \mathbf{h}_m^T\mathbf{d}(k), \tag{8}$$

where $\mathbf{U}_{sa}(k) = [\mathbf{u}_{sa}(k-1) \ \mathbf{u}_{sa}(k-2) \ \cdots \ \mathbf{u}_{sa}(k-P)]$, $\mathbf{u}_{sa}(k-l) = [u(k-l) \ u(k-l-1) \ \cdots \ u(k-l-L+1)]^T$, $\mathbf{f}_s(k) = [f(k) \ f(k-1) \ \cdots \ f(k-L+1)]^T$, and L is the length of analysis filters. The notation $(\downarrow M)$ means a decimation by M. Note that the decimated signals $u_{mn}(k) = u_m(Mk-n)$ and $f_{mn}(k) = f_m(Mk-n)$ are the subband polyphase components of $u_m(k)$ and $f_m(k)$, respectively.

These subband polyphase component vectors can be presented by

$$\mathbf{u}_{mn}(k) = \left[u_{mn}(k) \;\; u_{mn}(k-1) \;\; \cdots \;\; u_{mn}(k-Ps)\right]^T,$$
$$\mathbf{f}_{mn}(k) = \left[f_{mn}(k) \;\; f_{mn}(k-1) \;\; \cdots \;\; f_{mn}(k-Ps)\right]^T, \tag{9}$$

where the subscript mn is the subband-decomposed polyphase index (m and $n = 0, 1, \ldots, M-1$). In M-subband structure, the adaptive filter can be represented in terms of polyphase components as

$$\mathbf{S}(z) = \mathbf{S}_0(z^M) + z^{-1}\mathbf{S}_1(z^M) + \cdots + z^{-i}\mathbf{S}_i(z^M). \tag{10}$$

Based on the principle of minimum disturbance [2] and the criterion of (4) for the fullband AP adaptive filter, we formulate a criterion for the M-subband AP filters as one of optimization subject to multiple constraints, as follows:

$$\begin{aligned}&\text{minimize } f[\mathbf{s}(k)] = \left\|\mathbf{s}_0(k+1) - \mathbf{s}_0(k)\right\|^2 \\ &\qquad + \cdots + \left\|\mathbf{s}_{M-1}(k+1) - \mathbf{s}_{M-1}(k)\right\|^2 \\ &\text{subject to } \mathbf{d}_m(k) = \sum_{n=0}^{M-1} \mathbf{U}_{mn}^T(k)\mathbf{s}_n(k+1) \\ &\qquad \text{for } m = 0, 1, \ldots, M-1.\end{aligned} \tag{11}$$

From this criterion, we define the cost function for the AP algorithm in the two-subband ($M = 2$) structure shown in Figure 3 as

$$\begin{aligned}J(k) &= \left\|\mathbf{s}_0(k+1) - \mathbf{s}_0(k)\right\|^2 + \left\|\mathbf{s}_1(k+1) - \mathbf{s}_1(k)\right\|^2 \\ &\quad + \left[\mathbf{d}_0(k) - \mathbf{U}_{00}^T(k)\mathbf{s}_0(k+1) - \mathbf{U}_{01}^T(k)\mathbf{s}_1(k+1)\right]^T\boldsymbol{\lambda}_0 \\ &\quad + \left[\mathbf{d}_1(k) - \mathbf{U}_{10}^T(k)\mathbf{s}_0(k+1) - \mathbf{U}_{11}^T(k)\mathbf{s}_1(k+1)\right]^T\boldsymbol{\lambda}_1,\end{aligned} \tag{12}$$

$$\mathbf{U}_{mn}(k) = \left[\mathbf{u}_{mn}(k) \;\; \mathbf{u}_{mn}(k-1) \;\; \cdots \;\; \mathbf{u}_{mn}(k-P_s)\right], \tag{13}$$

where $\boldsymbol{\lambda}_0$ and $\boldsymbol{\lambda}_1$ are the Lagrange multiplier vectors, and N_s and P_s are the length of the adaptive subfilter and the projection order in each subband, respectively. In (12), the cost function is quadratic, and also, it is convex since its Hessian matrix is positive definite [2, 23]. Therefore, the proposed cost function has a global minimum solution. From (12), we can get the partial derivatives of the cost function with respect to $\mathbf{s}_0(k+1)$ and $\mathbf{s}_1(k+1)$, and set the results to zeroes as [2]

$$\begin{aligned}&\frac{\partial J(k)}{\partial \mathbf{s}_0(k+1)} \\ &\quad = 2\left[\mathbf{s}_0(k+1) - \mathbf{s}_0(k)\right] - \mathbf{U}_{00}(k)\boldsymbol{\lambda}_0 - \mathbf{U}_{10}(k)\boldsymbol{\lambda}_1 = 0, \\ &\frac{\partial J(k)}{\partial \mathbf{s}_1(k+1)} \\ &= 2\left[\mathbf{s}_1(k+1) - \mathbf{s}_1(k)\right] - \mathbf{U}_{01}(n)\boldsymbol{\lambda}_0 - \mathbf{U}_{11}(n)\boldsymbol{\lambda}_1 = 0.\end{aligned} \tag{14}$$

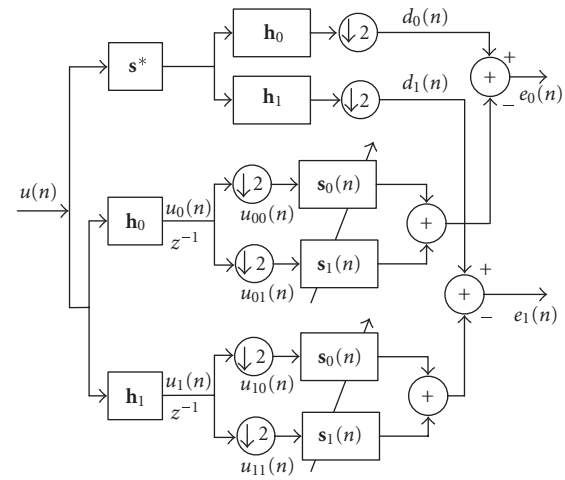

Figure 3: System identification model for two-subband adaptive filter.

To find the Lagrange vectors $\boldsymbol{\lambda}_0$ and $\boldsymbol{\lambda}_1$ that minimize the cost function of (12) with respect to $\mathbf{s}_0(k+1)$ and $\mathbf{s}_1(k+1)$, the error vectors in each subband are expressed as

$$\begin{aligned}\mathbf{e}_0(k) &= \frac{1}{2}\left[\mathbf{U}_{00}^T(k)\mathbf{U}_{00}(k) + \mathbf{U}_{01}^T(k)\mathbf{U}_{01}(k)\right]\boldsymbol{\lambda}_0 \\ &\quad + \frac{1}{2}\left[\mathbf{U}_{00}^T(k)\mathbf{U}_{10}(k) + \mathbf{U}_{01}^T(k)\mathbf{U}_{11}(k)\right]\boldsymbol{\lambda}_1, \\ \mathbf{e}_1(k) &= \frac{1}{2}\left[\mathbf{U}_{10}^T(k)\mathbf{U}_{00}(k) + \mathbf{U}_{11}^T(k)\mathbf{U}_{01}(k)\right]\boldsymbol{\lambda}_0 \\ &\quad + \frac{1}{2}\left[\mathbf{U}_{10}^T(k)\mathbf{U}_{10}(k) + \mathbf{U}_{11}^T(k)\mathbf{U}_{11}(k)\right]\boldsymbol{\lambda}_1.\end{aligned} \tag{15}$$

From (15), $\boldsymbol{\lambda}_0$ and $\boldsymbol{\lambda}_1$ can be represented in matrix form as

$$\begin{bmatrix}\boldsymbol{\lambda}_0 \\ \boldsymbol{\lambda}_1\end{bmatrix} = 2\begin{bmatrix}\mathbf{A}_0(k) & \mathbf{B}(k) \\ \mathbf{B}^T(k) & \mathbf{A}_1(k)\end{bmatrix}^{-1}\begin{bmatrix}\mathbf{e}_0(k) \\ \mathbf{e}_1(k)\end{bmatrix}, \tag{16}$$

where

$$\begin{aligned}\mathbf{A}_0(k) &= \mathbf{U}_{00}^T(k)\mathbf{U}_{00}(k) + \mathbf{U}_{01}^T(k)\mathbf{U}_{01}(k), \\ \mathbf{A}_1(k) &= \mathbf{U}_{10}^T(k)\mathbf{U}_{10}(k) + \mathbf{U}_{11}^T(k)\mathbf{U}_{11}(k),\end{aligned} \tag{17}$$

$$\mathbf{B}(k) = \mathbf{U}_{00}^T(k)\mathbf{U}_{10}(k) + \mathbf{U}_{01}^T(k)\mathbf{U}_{11}(k). \tag{18}$$

In (16), the matrix $\mathbf{B}(k)$ in the off-diagonal is an undesirable cross-term that is produced by the signals of different subbands. To eliminate this cross-term, we define $\mathbf{G}_m(k) = E\{\mathbf{A}_m(k)\}$ and $\mathbf{K}(k) = E\{\mathbf{B}(k)\}$ ($E\{\cdot\}$ denotes the expectation of $\{\cdot\}$). The matrix $\mathbf{G}_m(k)$ in the main diagonal is the sum of $P_s \times P_s$ Grammian matrices that consist of sample autocorrelations $\mathbf{R}_m(k)$ (for $m = 0$ or 1). Therefore, $\mathbf{G}_0(k)$ and

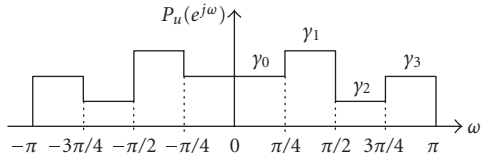

FIGURE 4: Sample power spectrum of $u(k)$.

$\mathbf{G}_1(k)$ can be written as

$$\begin{aligned}\mathbf{G}_0(k) &= E\{\mathbf{A}_0(k)\}\\ &= E\{\mathbf{U}_{00}^T(k)\mathbf{U}_{00}(k)+\mathbf{U}_{01}^T(k)\mathbf{U}_{01}(k)\}\\ &= \mathbf{R}_0(k)+\mathbf{R}_0(k-1)+\cdots+\mathbf{R}_0(k-N_s+1),\\ \mathbf{G}_1(k) &= E\{\mathbf{A}_1(k)\}\\ &= E\{\mathbf{U}_{10}^T(k)\mathbf{U}_{10}(k)+\mathbf{U}_{11}^T(k)\mathbf{U}_{11}(k)\}\\ &= \mathbf{R}_1(k)+\mathbf{R}_1(k-1)+\cdots+\mathbf{R}_1(k-N_s+1).\end{aligned} \tag{19}$$

Whereas, the matrix $\mathbf{K}(k)$ in the off-diagonal is the sum of $P_s \times P_s$ sample cross-correlations $\mathbf{C}(k)$ that consist of signals of different subband components. The matrix $\mathbf{K}(k)$ can be written as

$$\begin{aligned}\mathbf{K}(k) &= E\{\mathbf{B}(k)\}\\ &= E\{\mathbf{U}_{00}^T(k)\mathbf{U}_{10}(k)+\mathbf{U}_{01}^T(k)\mathbf{U}_{11}(k)\}\\ &= \mathbf{C}(k)+\mathbf{C}(k-1)+\cdots+\mathbf{C}(k-N_s+1).\end{aligned} \tag{20}$$

In (20), each element of $\mathbf{K}(k)$ can be obtained as a sum of inner products of different subband components. We can write each element as

$$\gamma_{\mathbf{u}_{00}\mathbf{u}_{10}+\mathbf{u}_{01}\mathbf{u}_{11}}(k,l) = E\{\mathbf{u}_{00}^T(k)\mathbf{u}_{10}(l)+\mathbf{u}_{01}^T(k)\mathbf{u}_{11}(l)\}. \tag{21}$$

Assuming that the input signal is wide-sense stationary and ergodic, the cross-correlation at zero lag, $\gamma_{\mathbf{u}_{00}\mathbf{u}_{10}+\mathbf{u}_{01}\mathbf{u}_{11}}(k,l)$, can be expressed as

$$\gamma_{\mathbf{u}_{00}\mathbf{u}_{10}+\mathbf{u}_{01}\mathbf{u}_{11}}(0) = \frac{[\mathbf{u}_{00}^T(k)\mathbf{u}_{10}(k)+\mathbf{u}_{01}^T(k)\mathbf{u}_{11}(k)]}{N_s}. \tag{22}$$

For analytical simplicity, we further assume that the input signal is white and its spectrum is flat in each subband as shown in Figure 4. From these assumptions, $E\{\mathbf{u}_{00}^T\mathbf{u}_{00}+\mathbf{u}_{01}^T\mathbf{u}_{01}\} = \sigma_{\mathbf{u}_0}^2$ ($\sigma_{\mathbf{u}_0}^2$ is the variance of subband signal $\mathbf{h}_0^T\mathbf{u}$) and $E\{\mathbf{u}_{00}^T\mathbf{u}_{10}+\mathbf{u}_{01}^T\mathbf{u}_{11}\} = 0$. For colored inputs, $E\{\mathbf{u}_{00}^T\mathbf{u}_{10}+\mathbf{u}_{01}^T\mathbf{u}_{11}\} \neq 0$. However, if the frequency responses of the analysis filters do not overlap significantly, it is always true that $E\{\mathbf{u}_{00}^T\mathbf{u}_{10}+\mathbf{u}_{01}^T\mathbf{u}_{11}\} \ll E\{\mathbf{u}_{00}^T\mathbf{u}_{00}+\mathbf{u}_{01}^T\mathbf{u}_{01}\}$ as before. This means that the elements of $\mathbf{B}(k)$ are very small compared with the elements of $\mathbf{A}_0(k)$ and $\mathbf{A}_1(k)$. Therefore, we can consider $\mathbf{B}(k) \approx \mathbf{0}$.

With the above approximations, (16) can be simplified as

$$\begin{aligned}\begin{bmatrix}\boldsymbol{\lambda}_0\\ \boldsymbol{\lambda}_1\end{bmatrix} &= 2\begin{bmatrix}\mathbf{A}_0(k) & \mathbf{B}(k)\\ \mathbf{B}^T(k) & \mathbf{A}_1(k)\end{bmatrix}^{-1}\begin{bmatrix}\mathbf{e}_0(k)\\ \mathbf{e}_1(k)\end{bmatrix}\\ &\approx 2\begin{bmatrix}\mathbf{A}_0(k) & \mathbf{0}\\ \mathbf{0} & \mathbf{A}_1(k)\end{bmatrix}^{-1}\begin{bmatrix}\mathbf{e}_0(k)\\ \mathbf{e}_1(k)\end{bmatrix}.\end{aligned} \tag{23}$$

From (17) and (23), the Lagrange vectors $\boldsymbol{\lambda}_0$ and $\boldsymbol{\lambda}_1$ are obtained as

$$\begin{aligned}\boldsymbol{\lambda}_0 &= 2\left[\mathbf{U}_{00}^T(k)\mathbf{U}_{00}(k)+\mathbf{U}_{01}^T(k)\mathbf{U}_{01}(k)\right]^{-1}\mathbf{e}_0(k),\\ \boldsymbol{\lambda}_1 &= 2\left[\mathbf{U}_{10}^T(k)\mathbf{U}_{10}(k)+\mathbf{U}_{11}^T(k)\mathbf{U}_{11}(k)\right]^{-1}\mathbf{e}_1(k).\end{aligned} \tag{24}$$

Substituting (24) into (14), we can obtain the weight updating formulae of the SAP algorithm in the two-subband case as follows:

$$\begin{aligned}&\mathbf{s}_0(k+1)\\ &\quad= \mathbf{s}_0(k)+\mu\left[\mathbf{U}_{00}(k)\mathbf{A}_0^{-1}(k)\mathbf{e}_0(k)+\mathbf{U}_{10}(k)\mathbf{A}_1^{-1}(k)\mathbf{e}_1(k)\right],\\ &\mathbf{s}_1(k+1)\\ &\quad= \mathbf{s}_1(k)+\mu\left[\mathbf{U}_{01}(k)\mathbf{A}_0^{-1}(k)\mathbf{e}_0(k)+\mathbf{U}_{11}(k)\mathbf{A}_1^{-1}(k)\mathbf{e}_1(k)\right].\end{aligned} \tag{25}$$

3.1. Extension to the M-subband case

To generalize (25), we consider the M-subband structure shown in Figure 2(b) [13]. The cost function for this case is defined as an extension of (12),

$$\begin{aligned}J(k) = \sum_{m=0}^{M-1}\Bigg(&||\mathbf{s}_m(k+1)-\mathbf{s}_m(k)||^2\\ &+\left[\mathbf{d}_m(k)-\sum_{n=0}^{M-1}\mathbf{U}_{mn}^T(k)\mathbf{s}_n(k+1)\right]^T\boldsymbol{\lambda}_m\Bigg)\\ &\text{for } M=2,3,\ldots.\end{aligned} \tag{26}$$

Using (25), the proposed weight updating formula for the M-subband case can be expressed in terms of the matrix forms as follows:

$$\mathbf{S}(k+1) = \mathbf{S}(k)+\mu\mathbf{X}(k)\boldsymbol{\Pi}^{-1}(k)\mathbf{E}(k), \tag{27}$$

where

$$\mathbf{S}(k) = \left[\mathbf{s}_0^T(k)\ \ \mathbf{s}_1^T(k)\ \ \cdots\ \ \mathbf{s}_{M-1}^T(k)\right]^T,$$

$$\mathbf{X}(k) = \begin{bmatrix}\mathbf{U}_{00}(k) & \mathbf{U}_{10}(k) & \cdots & \mathbf{U}_{(M-1)0}(k)\\ \mathbf{U}_{01}(k) & \mathbf{U}_{11}(k) & \cdots & \mathbf{U}_{(M-1)1}(k)\\ \vdots & \vdots & \ddots & \vdots\\ \mathbf{U}_{0(M-1)}(k) & \mathbf{U}_{1(M-1)}(k) & \cdots & \mathbf{U}_{(M-1)(M-1)}(k)\end{bmatrix},$$

$\mathbf{X}(k)$ is $MN_s \times MP_s$ matrix,

$$\mathbf{\Pi}(k) = \begin{bmatrix} \mathbf{A}_0(k) & \mathbf{0} & \cdots & \mathbf{0} \\ \mathbf{0} & \mathbf{A}_1(k) & & \vdots \\ \vdots & & \ddots & \mathbf{0} \\ \mathbf{0} & \cdots & \mathbf{0} & \mathbf{A}_{(M-1)}(k) \end{bmatrix}, \quad \mathbf{\Pi}(k) \text{ is } MP_s \times MP_s \text{ matrix},$$

$$\mathbf{E}(k) = \begin{bmatrix} \mathbf{e}_0(k) \\ \mathbf{e}_1(k) \\ \vdots \\ \mathbf{e}_{M-1}(k) \end{bmatrix}, \quad \mathbf{E}(k) \text{ is } MP_s \times 1 \text{ vector}. \tag{28}$$

3.2. The projection order reduced by signal partitioning

The AP algorithm of (6) is rewritten with a direction vector $\mathbf{\Phi}(k)$ as follows [24]:

$$\mathbf{s}(k+1) = \mathbf{s}(k) + \mu \frac{\mathbf{\Phi}(k)}{\mathbf{\Phi}^T(k)\mathbf{\Phi}(k)} \mathbf{e}(k), \tag{29}$$

$$\begin{aligned} \mathbf{\Phi}(k) &= \mathbf{u}(k) - \mathbf{U}_a(k)\hat{\mathbf{a}}(k), \\ \hat{\mathbf{a}}(k) &= \left[\mathbf{U}_a^T(k)\mathbf{U}_a(k)\right]^{-1}\mathbf{U}_a^T(k)\mathbf{u}(k). \end{aligned} \tag{30}$$

In (29), the AP algorithm updates the adaptive filter weights $\mathbf{s}(k)$ in direction of a vector $\mathbf{\Phi}(k)$. The direction vector is the error vector in estimation (in least-squares sense) and it is orthogonal to the last P input vectors. Similarly, in (27), the SAP algorithm updates the adaptive subfilter weights $\mathbf{s}_m(k)$ in direction of a vector $\mathbf{\Phi}_m(k)$ given by

$$\mathbf{\Phi}_m(k) = \sum_{m=0}^{M-1} \mathbf{\Phi}_{mn}(k), \tag{31}$$

where each subdirection vector for the adaptive subfilters is given by

$$\mathbf{\Phi}_{mn}(k) = \mathbf{u}_{mn}(k) - \mathbf{U}_{amn}(k)\hat{\mathbf{a}}_{mn}(k), \tag{32}$$

$$\hat{\mathbf{a}}_{mn}(k) = \left[\mathbf{U}_{amn}^T(k)\mathbf{U}_{amn}(k)\right]^{-1}\mathbf{U}_{amn}^T(k)\mathbf{u}_{mn}(k), \tag{33}$$

$$[4pt]\mathbf{U}_{amn}(k) = \left[\mathbf{u}_{mn}(k-1)\ \ \mathbf{u}_{mn}(k-2)\ \ \cdots\ \ \mathbf{u}_{mn}(k-P_s)\right]. \tag{34}$$

In (33), $\hat{\mathbf{a}}_{mn}(k)$ is the subband least-squares estimate of the parameter vector $\mathbf{a}$, and it is transformed by orthogonal subband filtering. $\mathbf{\Phi}_{mn}(k)$ is orthogonal to the past P_s input vectors $\mathbf{u}_{mn}(k-1), \mathbf{u}_{mn}(k-2), \ldots, \mathbf{u}_{mn}(k-P_s)$. From (31) and (32), we can know that the weights of the adaptive subfilter are updated to the orthogonal direction of the past MP_s decomposed subband input vectors. In the fullband AP algorithm, AR(P) input signal is decorrelated by the projection matrix as shown in (7). Similarly, each subband input signal is decorrelated by the subband projection matrices as follows:

$$\mathbf{P}_{U_{amn}}(k) = \mathbf{U}_{amn}(k)\left[\mathbf{U}_{amn}^T(k)\mathbf{U}_{amn}(k)\right]^{-1}\mathbf{U}_{amn}^T(k). \tag{35}$$

To decorrelate the AR(P) input signal, the fullband AP algorithm performs the P times projection operations with the corresponding past P input vectors. In the proposed method, on the other hand, the projection operation with lower order ($P_s < P$) is sufficient for the signal decorrelating. Because the input signal is prewhitened by the subband partitioning, therefore, the spectral dynamic range of each subband signal is decreased. Moreover, the length of the adaptive subfilter becomes $N_s = N/M$ by applying the polyphase decomposition and the noble identity to the maximally decimated adaptive filter. In weight updating of AP adaptive filter, the order of projection governs the convergence rate of adaptive algorithm and it depends on the length of the AP adaptive filter as well as the degree of the input correlation. A high order of projection is required for the long adaptive filter, whereas, lower order of projection is sufficient for the shortened adaptive filter. Therefore, the projection order for the shortened adaptive subfilter can be $P_s \approx P/M$. When the size of the data matrix is $N \times (P+1)$ in the fullband, it can be $N_s \times (P_s+1) \approx (N/M) \times (P/M)$ in the subband. Moreover, in view of the computational complexity of the SAP, the weights of the adaptive subfilters in the subband structure are updated at a low rate that is provided by maximal decimation. Consequently, computational complexity of the proposed method is much less than that of fullband AP.

Now, we consider a simple implementation technique of the proposed SAP. Although a computational complexity of the proposed method is reduced, it still remains the inversion problem of matrix. In the AP algorithm, the projection order is typically much smaller than the length of the adaptive filter. By partitioning the P-order fullband AP into P-subbands, we obtain the simplified SAP (SSAP) with $N/P \times 1$ data vectors for weight updating instead of data matrices. Consequently, the weight updating formula for each subband adaptive subfilter is similar to that of the NLMS adaptive filter and the matrix inversion is not required. Now, we assume that the projection order in the fullband is 2 ($P = 2$). By partitioning into two-subbands, (25) are simply rewritten as

$$\begin{aligned} \mathbf{s}_0(k+1) &= \mathbf{s}_0(k) + \mu\left[\frac{\mathbf{u}_{00}(k)e_0(k)}{\sigma^2_{\mathbf{u}_0}(k)} + \frac{\mathbf{u}_{10}(k)e_1(k)}{\sigma^2_{\mathbf{u}_1}(k)}\right], \\ \mathbf{s}_1(k+1) &= \mathbf{s}_1(k) + \mu\left[\frac{\mathbf{u}_{01}(n)e_0(k)}{\sigma^2_{\mathbf{u}_0}(k)} + \frac{\mathbf{u}_{11}(k)e_1(k)}{\sigma^2_{\mathbf{u}_1}(k)}\right], \end{aligned} \tag{36}$$

where $\sigma^2_{\mathbf{u}_m}(k)$ is the variance of input signal in each subband.

Note that the computational complexity for the subband partitioning is much less than that for calculating the inverse matrix. In a practical implementation, the SSAP gives considerable savings in computational complexity.

3.3. Convergence of the mean weight vector

To analyze the convergence behavior of the proposed SAP, we first define the mean-square deviation as

$$D(k) = E\{||\tilde{\mathbf{s}}(k)||^2\} = E\{||\mathbf{s}^* - \mathbf{s}(k)||^2\}. \tag{37}$$

Table 1: Comparison of the computational complexities; N is the length of adaptive filter or unknown system (filter), L is the length of analysis and synthesis filters, M is the number of subbands, P is the projection order, and D is the size of data frame in LC-GSFAP.

Algorithms	Multiplications/iteration	Multiplications/iteration for $L = 64$, $N = 512$, $M = 4$, $P = 4$, $D = 2$
SNLMS [13]	$3N + 2M(L + 2)$	2064
Fullband AP [3]	$P^3/2 + 3NP^2 + NP + N$	27 168
Subband LC-GSFAP [19]	$M(P^2 + P + N + (2P + N)/D + 1)$ $+2ML$	3160
The proposed SAP	$P^3/(2M^3) + NP^2(M + 1)/M^3$ $+NP(P + M + 1)/M^2 + 2ML$	$\approx$ 2305
The SSAP	$3N + 2P(L + 2)$	2064

For analytical simplicity, we consider the two-subband case. The polyphase components of the unknown filter, $\mathbf{s}_0^*$ and $\mathbf{s}_1^*$, can be represented as

$$\mathbf{S}^*(z) = \mathbf{S}_0^*(z^2) + z^{-1}\mathbf{S}_1^*(z^2). \tag{38}$$

From (27), we can get

$$\widetilde{\mathbf{S}}(k+1) = \widetilde{\mathbf{S}}(k) - \mu\mathbf{X}(n)\mathbf{\Pi}^{-1}(k)\mathbf{E}(k), \tag{39}$$

where $\widetilde{\mathbf{S}}(k) = [\widetilde{\mathbf{s}}_0^T(k)\ \ \widetilde{\mathbf{s}}_1^T(k)]^T$, for $\widetilde{\mathbf{s}}_0(k) = \mathbf{s}_0^* - \mathbf{s}_0(k)$ and $\widetilde{\mathbf{s}}_1(k) = \mathbf{s}_1^* - \mathbf{s}_1(k)$. Taking the squared-Euclidean norm on both sides of (39), the weight updating formula can be represented as (assume that $\mathbf{X}^T(k)\mathbf{X}(k) \approx \mathbf{\Pi}(k)$)

$$\begin{aligned}&||\widetilde{\mathbf{S}}(k+1)||^2 - ||\widetilde{\mathbf{S}}(k)||^2\\ &\quad= \mu^2\mathbf{E}^T(k)\mathbf{\Pi}^{-1}(k)\mathbf{E}(k) - 2\mu||\widetilde{\mathbf{S}}^T(k)\mathbf{X}(k)\mathbf{\Pi}^{-1}(n)\mathbf{E}(k)||,\end{aligned} \tag{40}$$

and taking the expectation on both sides of (40), we can get

$$\begin{aligned}&D(k+1) - D(k)\\ &\quad= \mu^2 E\{\mathbf{E}^T(k)\mathbf{\Pi}^{-1}(k)\mathbf{E}(k)\} - 2\mu E\{||\boldsymbol{\xi}(k)\mathbf{\Pi}^{-1}(k)\mathbf{E}(k)||\},\end{aligned} \tag{41}$$

where

$$\boldsymbol{\xi}(k) = \widetilde{\mathbf{S}}^T(k)\mathbf{X}(k). \tag{42}$$

For the proposed algorithm to be stable, the mean-square deviation $D(k)$ must decrease monotonically with an increasing number of iterations n implying that $D(k+1) - D(k) < 0$. Therefore, the step size μ has to fulfill the condition

$$0 < \mu < \frac{2E\{||\boldsymbol{\xi}(k)\mathbf{\Pi}^{-1}(k)\mathbf{E}(k)||\}}{E\{\mathbf{E}^T(k)\mathbf{\Pi}^{-1}(k)\mathbf{E}(k)\}}. \tag{43}$$

In (43), $\boldsymbol{\xi}(k) = \widetilde{\mathbf{S}}^T(k)\mathbf{X}(k)$ is the undisturbed error vector. If we consider the situation where the disturbance is negligible, the disturbed error vector is equal to the error vector $\mathbf{E}^T(k)$. Hence, in the absence of disturbance, the necessary and sufficient condition for the convergence in the mean-square sense is that the step-size parameter must satisfy the double inequality

$$0 < \mu < 2. \tag{44}$$

3.4. Computational complexity

The computational complexities per iteration in terms of the number of multiplications for the proposed SAP and the SSAP, the fullband AP [3], the subband NLMS (SNLMS) [13], and the subband LC-GSFAP [19] are shown in Table 1. When the fullband sampling rate is $F_s = 1/T_s$, the weights of the adaptive filter in the subband structure are updated at a lower rate, $1/MT_s$. In the AP and the SAP, matrix inversions were assumed to be performed with standard LU decomposion: $O^3/2$ multiplications [17], where O is the rank of a square matrix, and it is equal to the projection order in AP ($O = P$ or P_s). In SSAP that partitioned into P-subband, the length of the subband adaptive filter is $N_s = N/M|_{M=P} = N/P$ and the projection order in each subband is $P_s = P/M|_{M=P} = 1$. In applications, such as adaptive echo cancellation, the length of analysis filters is typically much smaller than the length of the adaptive filter. Consequently, it can be seen that the proposed algorithm is much more efficient than the other algorithms.

4. SIMULATION RESULTS

To evaluate the performance of the proposed SAP algorithm, we carry out computer simulations in acoustic echo cancellation scenario. The length of the unknown system shown in Figure 5 is $N = 512$. It is an actual impulse response of the echo path in a room, sampled at 8 kHz and truncated to 512 samples. For signal partitioning in all experiments, we use the cosine-modulated filter banks [25] (analysis and synthesis) with prototype frequency responses shown in Figure 6.

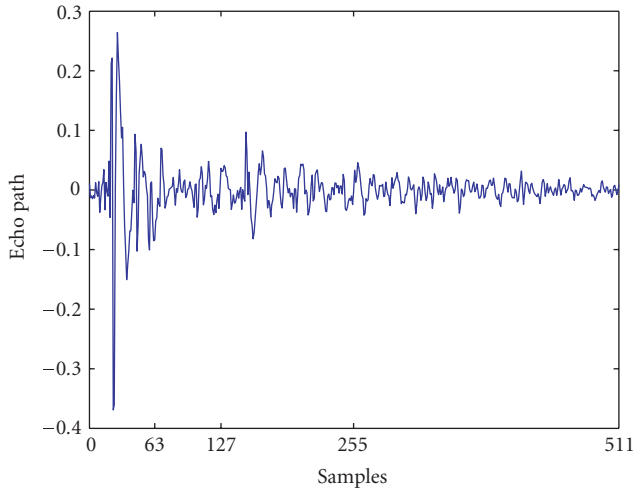

Figure 5: Impulse response of the echo path measured in a room.

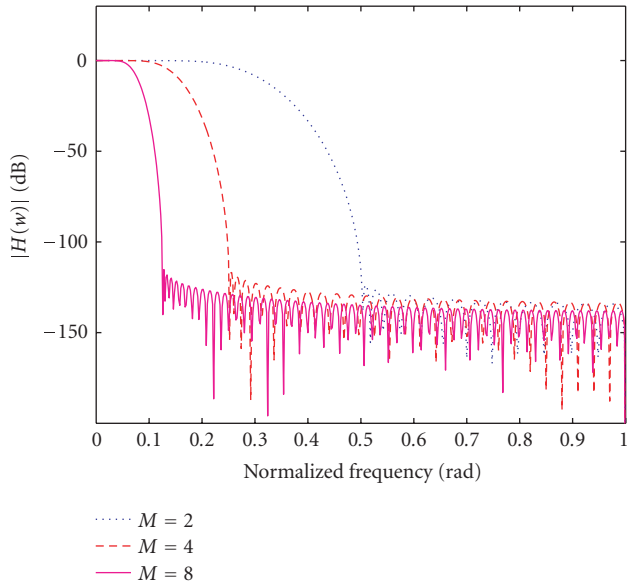

Figure 6: Frequency responses of the prototype filters.

For efficient subband decomposition of input signals, the lengths of analysis filters are increased with M so that the ratio of the transition band to the passband is maintained nearly the same for all values of M. The prototype filters' lengths are 32, 64, and 128 for $M = 2, 4$, and 8, respectively. The input signals are zero-mean wide-sense stationary AR(P) and a real speech sampled at 8 kHz. AR(4) process is given by

$$u(k) = \sum_{l=1}^{P} a_l u(k-l) + f(k), \tag{45}$$

where AR coefficients are $\mathbf{a} = [1 \;\; 0.999 \;\; 0.99 \;\; 0.995 \;\; 0.9]^T$ for AR(4). $f(k)$ is zero-mean and unit-variance white Gaussian random process. The measurement noise is added to

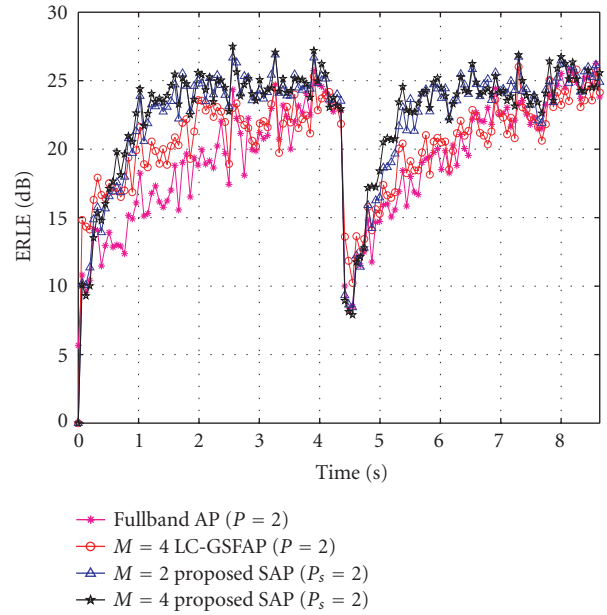

Figure 7: ERLE curves of the fullband AP with $P = 2$, $M = 4$ LC-GSFAP with $P = 2$ and $D = 2$, $M = 2$ SAP with $P_s = 2$, and $M = 4$ SAP with $P_s = 2$ for AR(4) inputs ($N = 512$, $\mu = 1$, SNR = 30 dB).

desire signal $d(k)$ such that SNR = 30 dB. The step size is set to a unit ($\mu = 1$) for fast convergence. In acoustic echo cancellation systems as shown in Figures 1 and 2, we evaluate the echo return loss enhancement (ERLE) performances of the proposed SAP, the fullband AP, and the four-subband LC-GSFAP with 2-oversampling factor (OS = 2) algorithm.

$$\text{ERLE} = 10\log_{10}\left(\frac{\sum_{i=0}^{N-1} d^2(n-i)}{\sum_{i=0}^{N-1} e^2(n-i)}\right). \tag{46}$$

Generally, the weights of adaptive filter are frozen when the double talk is detected, then they are readjusted when the double talk is inactive. For the double-talk condition, we evaluate the tracking ability of the proposed method. The path of echo is changed at the detected time and the weights of adaptive filter are frozen and then, when the double talk is inactive, the weights of adaptive filter are readjusted to cancel the changed echo path.

4.1. The proposed SAP with AR(4) input

Figure 7 shows the ERLE performances of the proposed method, the fullband AP, and subband LC-GSFAP with the same projection order ($P = P_s = 2$) for different numbers of subbands ($M = 2, 4$). We assumed that the double talk is detected at about 4.5 (seconds). For the same projection order, the SAP and the subband LC-GSFAP have faster convergence rates than the fullband. From these results, we can doubtlessly know that the convergence speed of adaptive filter is improved by the subband filtering and it speeds up with the increase of M. Figure 8 shows the ERLE of each algorithm with the different values of the projection order ($P = 4$

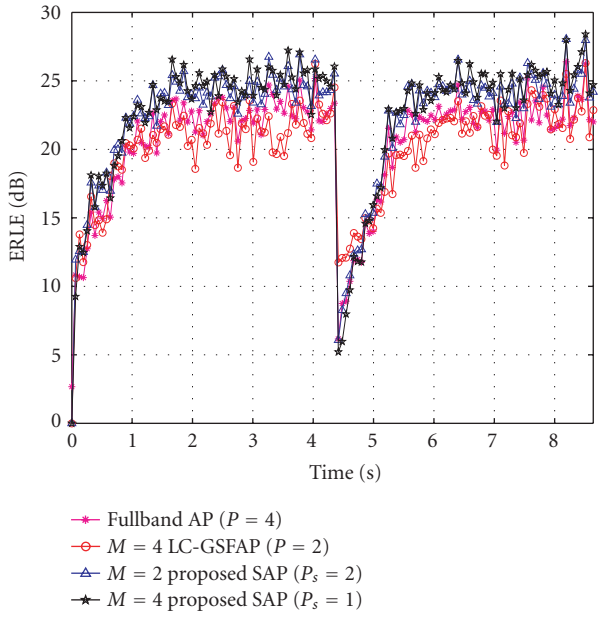

Figure 8: ERLE curves of the fullband AP with $P = 4$, $M = 4$ LC-GSFAP with $P = 2$, OS $= 2$, and $D = 2$, $M = 2$ SAP with $P_s = 2$, and $M = 4$ SAP with $P_s = 1$ for AR(4) inputs ($N = 512$, $\mu = 1$, SNR $= 30$ dB).

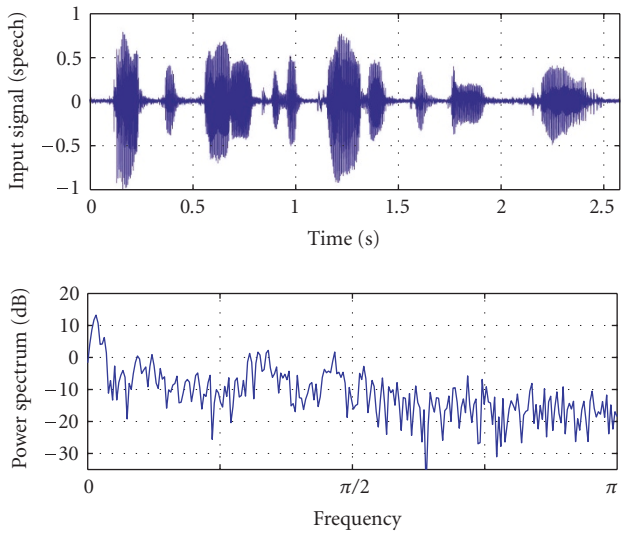

Figure 9: Input signal (speech) and its power spectrum of speech ($f_s = 8$ kHz).

and $P_s = 1, 2$) and different numbers of subbands ($M = 2, 4$). Comparing the results of Figure 8 with that of Figure 7, the convergence speeds of the SAP with the reduced projection order can be deteriorated. However, it is faster than that of other algorithms. From these results, the increase of M improves the convergence speed and also allows the projection order P to be reduced. Therefore, it can be said that the proposed SAP improves the performance of the conventional AP in the efficiency. Consequently, the SAP is superior to other

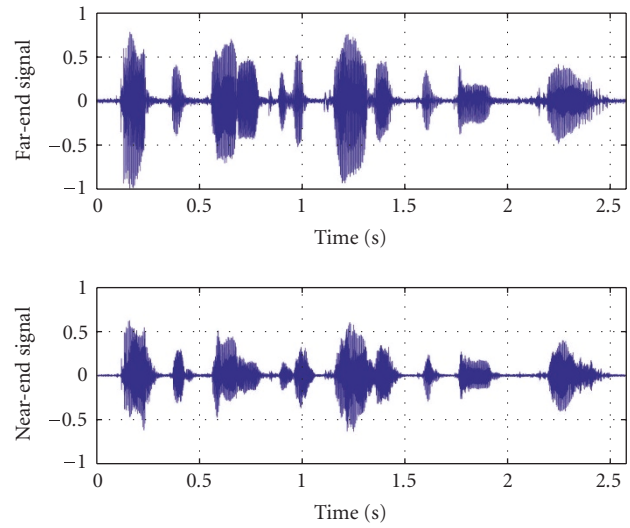

Figure 10: Far-end signal and near-end signal of AEC with speech as excitation.

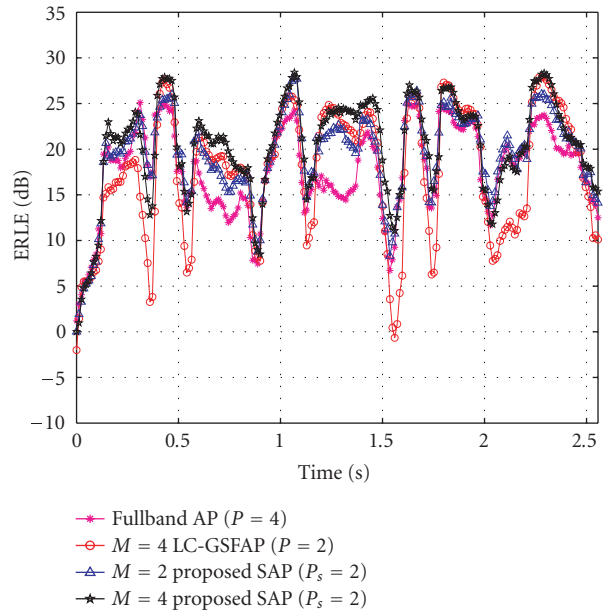

Figure 11: Comparison of ERLE for fullband AP, $M = 4$, OS $= 2$, and $D = 2$ LC-GSFAP, $M = 2$ SAP, and $M = 4$ SAP with 8 kHz sampled speech as excitation ($N = 512$, $P = P_s = 2$, $\mu = 1$, SNR $= 30$ dB).

algorithms in view of the computational complexity and the convergence speed.

4.2. The proposed SAP with real speech input

The speech signal and its power spectrum are shown in Figure 9. The speech is a woman's voice sampled at 8 kHz. Figure 10 shows the far-end signal and the near-end signal of AEC. The projection orders for each algorithm are equal to 2 ($P = P_s = 2$). The speaker output signal-to-measurement noise is set to 30 dB. Figure 11 shows ERLE curves of the

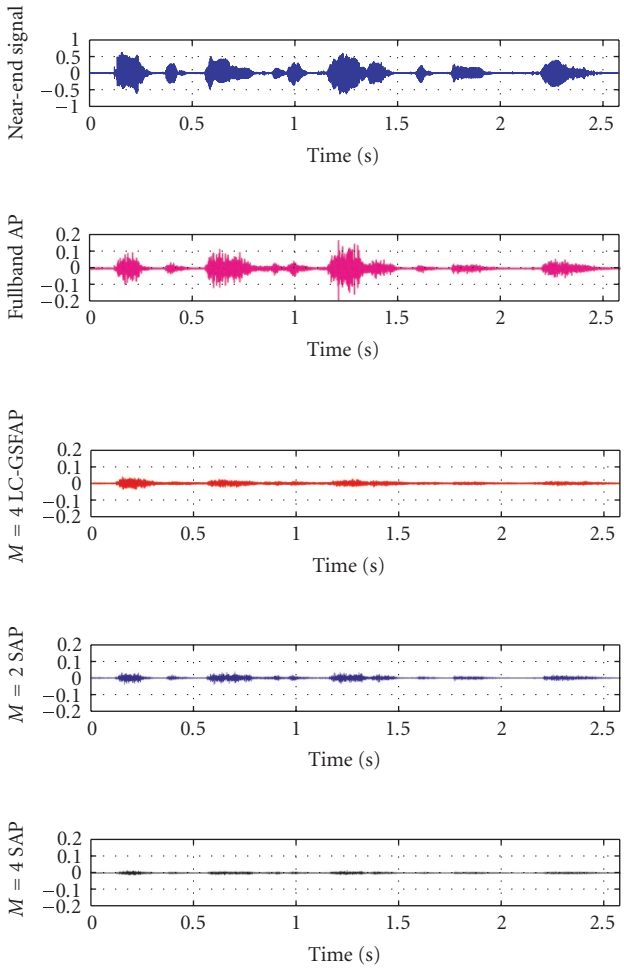

Figure 12: Comparison of residual error signals for Fullband AP, $M = 4$, OS $= 2$, and $D = 2$ LC-GSFAP, $M = 2$ SAP, and $M = 4$ SAP with speech as excitation ($N = 512$, $P = P_s = 2$, $\mu = 1$, SNR $= 30$ dB).

$M = 2, 4$ SAP, the $M = 4$, OS $= 2$ LC-GSFAP, and the fullband AP with the real speech as excitation. Figure 12 illustrates the residual error signal of each algorithm.

4.3. MSE performance of the SAP and the simplified SAP

We compare the performance of the proposed algorithms (the SAP and the SSAP) with other algorithms. Figure 13 shows the MSE curves of the SAP and the fullband AP. The convergence rate of the fullband AP goes up with P and those of the SAP go up with P or M. Increase of P leads to a large computational complexity, whereas, increase of M does not. For the same projection order, the SAP has faster convergence rates than the fullband. To evaluate the performance of the SSAP, two sets of simulations are considered. In the first set, the number of subbands in the SSAP and the projection order for the fullband AP are set to 4 ($M = 4$ and $P = 4$), whereas, those are 8 ($M = 8$ and $P = 8$) in the second set.

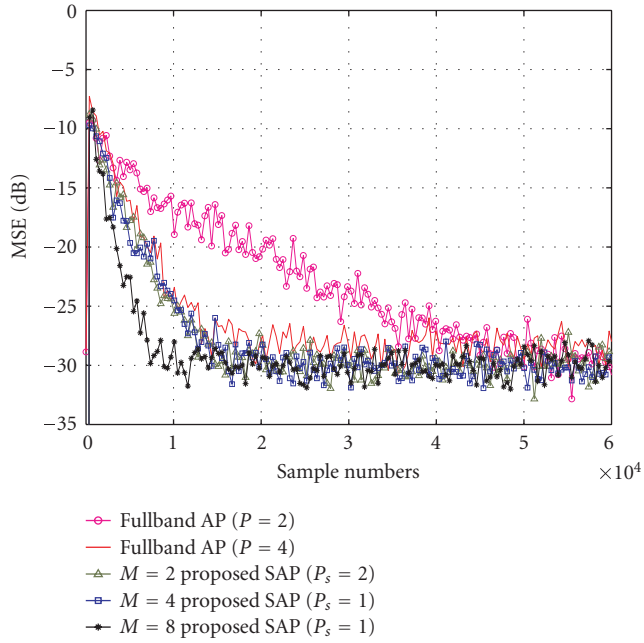

Figure 13: Comparison of MSE curves of the simplified SAP (SSAP) for AR(4) ($N = 512$, $\mu = 1$, SNR $= 30$ dB).

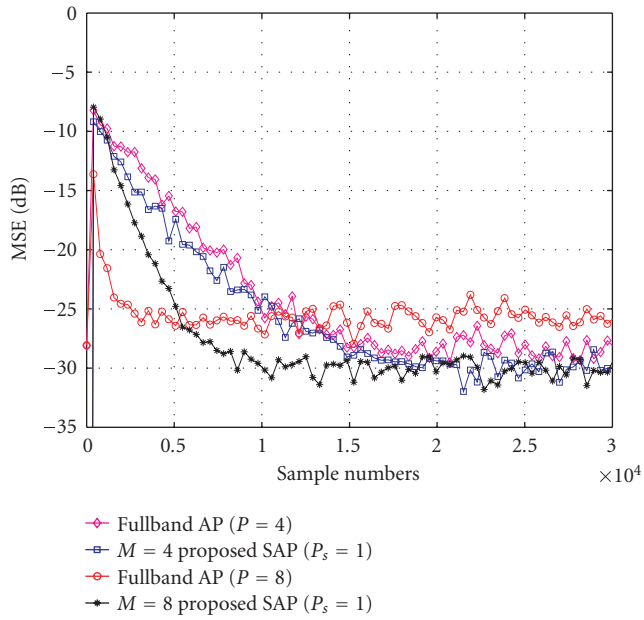

Figure 14: Comparison of MSE curves of each algorithm for AR(4) ($N = 512$, $\mu = 1$, SNR $= 30$ dB).

The projection order of the SSAP is 1 ($P_s = 1$) at both sets. Figure 14 shows the MSE curves of the SSAP and the fullband AP. In the first set, the convergence rate of the SSAP is similar to that of the fullband AP. In the second set, we can observe that the fullband AP is superior to the SSAP. However, the steady-state error of the fullband AP is larger than that of the SSAP. This large steady-state error is in accord with the result

of [24]. Moreover, as described earlier, the fullband AP with higher projection order has extremely large computational complexity. Whereas, the SSAP is comparable in view of the computational complexity with the NLMS. Consequently, we can conclude that the effect of the plenty subband partitioning is more effective than that of higher projection order to improve the convergence rate of the fullband AP.

5. CONCLUSIONS

In this paper, we present a new subband affine projection algorithm based on the subband structure [13] and the fullband affine projection algorithm [3] for acoustic echo cancellation. The proposed algorithm uses the OSF for prewhitening the highly correlated inputs. This OSF is a kind of projection operation and it can partly substitute for the updating-projection scheme of the fullband AP algorithm. Moreover, the OSF with the polyphase decomposition, the noble identity, and critical decimation can reduce the computational complexity. By combining the merits of the OSF and the AP algorithm, the derived method gives the rapid convergence rate and the reduced computational complexity. In addition, we present that the proposed algorithm can be reduced to a simplified form such as the NLMS by partitioning over the number of subbands as the projection order. The simplified form is a good approach to implement the proposed method in most practical applications. Several simulation results support the theoretical predictions and show the improved performances.

REFERENCES

[1] B. Widrow and S. D. Stearns, *Adaptive Signal Processing*, Prentice-Hall, Englewood Cliffs, NJ, USA, 1985.

[2] S. Haykin, *Adaptive Filter Theory*, Prentice-Hall, Upper Saddle River, NJ, USA, 4th edition, 2002.

[3] K. Ozeki and T. Umeda, "An adaptive filtering algorithm using an orthogonal projection to an affine subspace and its properties," *Electronics & Communications in Japan*, vol. 67, no. 5, pp. 19–27, 1984.

[4] S. G. Sankaran and A. A. Beex, "Convergence behavior of affine projection algorithms," *IEEE Transactions on Signal Processing*, vol. 48, no. 4, pp. 1086–1096, 2000.

[5] S. L. Gay and J. Benesty, *Acoustic Signal Processing for Telecommunication*, Kluwer Academic, Boston, Mass, USA, 2000.

[6] M. Rupp, "A family of adaptive filter algorithms with decorrelating properties," *IEEE Transactions on Signal Processing*, vol. 46, no. 3, pp. 771–775, 1998.

[7] S. Werner and P. S. R. Diniz, "Set-membership affine projection algorithm," *IEEE Signal Processing Letters*, vol. 8, no. 8, pp. 231–235, 2001.

[8] H.-C. Shin and A. H. Sayed, "Mean-square performance of a family of affine projection algorithms," *IEEE Transactions on Signal Processing*, vol. 52, no. 1, pp. 90–102, 2004.

[9] S. L. Gay and S. Tavathia, "The fast affine projection algorithm," in *Proceedings of the IEEE International Conference on Acoustics, Speech, and Signal Processing (ICASSP '95)*, vol. 5, pp. 3023–3026, Detroit, Mich, USA, May 1995.

[10] M. Tanaka, S. Makino, and J. Kojima, "A block exact fast affine projection algorithm," *IEEE Transactions on Speech and Audio Processing*, vol. 7, no. 1, pp. 79–86, 1999.

[11] F. Albu and H. K. Kwan, "Fast block exact Gauss-Seidel pseudo affine projection algorithm," *Electronics Letters*, vol. 40, no. 22, pp. 1451–1453, 2004.

[12] P. P. Vaidyanathan, *Multirate Systems and Filter Banks*, Prentice-Hall, Englewood Cliffs, NJ, USA, 1993.

[13] S. S. Pradhan and V. U. Reddy, "A new approach to subband adaptive filtering," *IEEE Transactions on Signal Processing*, vol. 47, no. 3, pp. 655–664, 1999.

[14] M. R. Petraglia, R. G. Alves, and P. S. R. Diniz, "New structures for adaptive filtering in subbands with critical sampling," *IEEE Transactions on Signal Processing*, vol. 48, no. 12, pp. 3316–3327, 2000.

[15] S. Miyagi and H. Sakai, "Convergence analysis of alias-free subband adaptive filters based on a frequency domain technique," *IEEE Transactions on Signal Processing*, vol. 52, no. 1, pp. 79–89, 2004.

[16] S. Makino, K. Strauss, S. Shimauchi, Y. Haneda, and A. Nakagawa, "Subband streo echo canceller using the projection algorithm with convergence to the true echo path," in *Proceedings of the IEEE International Conference on Acoustics, Speech, and Signal Processing (ICASSP '97)*, vol. 1, pp. 299–302, Munich, Germany, April 1997.

[17] M. Bouchard, "Multichannel affine and fast affine projection algorithms for active noise control and acoustic equalization systems," *IEEE Transactions on Speech and Audio Processing*, vol. 11, no. 1, pp. 54–60, 2003.

[18] Q. G. Liu, B. Champagne, and K. C. Ho, "On the use of a modified fast affine projection algorithm in subbands for acoustic echo cancelation," in *Proceedings of the IEEE Digital Signal Processing Workshop*, pp. 354–357, Loen, Norway, September 1996.

[19] E. Chau, H. Sheikhzadeh, and R. L. Brennan, "Complexity reduction and regularization of a fast affine projection algorithm for oversampled subband adaptive filters," in *Proceedings of the IEEE International Conference on Acoustics, Speech and Signal Processing (ICASSP '04)*, vol. 5, pp. 109–112, Montreal, Quebec, Canada, May 2004.

[20] K. Nishikawa and H. Kiya, "New structure of affine projection algorithm using a novel subband adaptive system," in *Proceedings of the 3rd IEEE Workshop on Signal Processing Advances in Wireless Communications (SPAWC '01)*, pp. 364–367, Taoyuan, Taiwan, March 2001.

[21] H. R. Abutalebi, H. Sheikhzadeh, R. L. Brennan, and G. H. Freeman, "Affine projection algorithm for oversampled subband adaptive filters," in *Proceedings of the IEEE International Conference on Acoustics, Speech and Signal Processing (ICASSP '03)*, vol. 6, pp. 209–212, Hong Kong, April 2003.

[22] E. K. P. Chong and S. H. Zak, *An Introduction to Optimization*, John Wiley & Sons, New York, NY, USA, 1996.

[23] T. K. Moon and W. C. Stirling, *Mathematical Methods and Algorithms*, Prentice-Hall, Englewood Cliffs, NJ, USA, 2000.

[24] S. J. M. de Almeida, J. C. M. Bermudez, N. J. Bershad, and M. H. Costa, "A statistical analysis of the affine projection algorithm for unity step size and autoregressive inputs," *IEEE Transactions on Circuits and Systems I: Regular Papers*, vol. 52, no. 7, pp. 1394–1405, 2005.

[25] Y.-P. Lin and P. P. Vaidyanathan, "A kaiser window approach for the design of prototype filters of cosine modulated filterbanks," *IEEE Signal Processing Letters*, vol. 5, no. 6, pp. 132–134, 1998.

Hun Choi received the B.S. and the M.S. degrees in electronics from Chungbuk National University, South Korea, in 1996 and 2001, respectively. Since 2001, he is currently pursuing the Ph.D. degree. From November 1996 to March 1997, he served as a Research Engineer in the Department of Product Development of LG Semicon. His research interests include adaptive signal processing, multirate signal processing, and methods applied to acoustic and communication systems.

Hyeon-Deok Bae received his M.S. and Ph.D. degrees in electronics from Seoul National University (SNU), South Korea, in 1980 and 1992, respectively. From 1983 to 1987, he was an Assistant Professor at Kwandong University, Kangwon, South Korea. Since 1987, he has been a Professor at Chungbuk National University, South Korea. His research interests include adaptive signal processing, multirate systems, and wavelets applications for signal processing. In 1994, he was a visiting Professor at Syracuse University, Syracuse, NY, USA.